

On Super-Resolution With an Experimental Microwave Tomography System

Colin Gilmore, *Member, IEEE*, Puyan Mojabi, *Student Member, IEEE*, Amer Zakaria, *Student Member, IEEE*, Stephen Pistorius, *Senior Member, IEEE*, and Joe LoVetri, *Senior Member, IEEE*

Abstract—The resolution of an experimental microwave tomography (MWT) system is investigated. Using two cylindrical nylon targets and an operating frequency of 5 GHz, a separation resolution of 2 mm, or 1/30 of a wavelength, is achieved. While this resolution is among the highest reported in the literature, it is not a sufficiently robust indicator of the expected resolution obtainable for complex targets, and this is shown with further examples of more complicated targets. However, the basic separation resolution limit obtained is a good way of comparing various aspects of different MWT systems.

Index Terms—Electromagnetic tomography, image resolution, microwave imaging.

I. INTRODUCTION

MICROWAVE tomography (MWT) is an imaging modality that uses electromagnetic radiation in the frequency range of a few hundred megahertz to a few gigahertz to quantitatively reconstruct the complex permittivity of the object being imaged. Biomedical MWT provides a promising alternative or complementary biomedical diagnostic technique to conventional soft-tissue imaging modalities. The advantages of MWT include its low cost, the use of nonionizing radiation, and the ability to quantitatively image the bulk electromagnetic properties of tissue (*i.e.*, the dielectric constant, as well as the conductivity of the tissue), which are not directly imaged by other modalities. Despite these advantages, MWT has not found a firm place as a clinical tool.

Perhaps the largest remaining challenge to make MWT a competitive biomedical imaging modality is to improve the achievable resolution over what has been reported for current state-of-the-art MWT systems, making it more comparable to MRI, ultrasound, and X-ray CT. The lower resolution of MWT is directly linked to the relatively larger wavelengths being used to interrogate the object of interest. There is, however,

no known theoretical limit to the spatial resolution obtainable from MWT; image resolution as low as 1/6 of a wavelength has been obtained for near-field imaging systems [1], and it has been suggested that the true resolution limit is governed by the achievable signal-to-noise ratio of the measurements [2] and not the wavelength (*cf.*, low-frequency impedance tomography systems [3]).

As the resolution limit for MWT technology is not currently known, and the future success of MWT depends upon improving the resolution performance of such systems, having a means of comparing the performance of different MWT systems (including the utilized data acquisition techniques, measurement calibration methods, and imaging algorithms) is important to the ongoing research effort in this area. In this letter, we quantify the resolution performance of our air-filled MWT system [4] by using a series of well-defined simple experiments designed to reveal the *separation resolution* limit of the system. The concept of separation resolution, though not identified as such, has been used before by other investigators as an indicator of their systems' performance and therefore allows for a comparison between systems. We show that the achievable separation resolution is much smaller than a half-wavelength, the Rayleigh limit, and is much better than previously published results. Some of the deficiencies in using the separation resolution as a way of measuring a systems' expected resolution performance are discussed and exemplified by examining images of more complicated targets. In the light of such examples, the scattering mechanisms responsible for the nonapplicability of the concept are reviewed, but it is concluded that, lacking other well-defined indicators of resolution performance applicable to MWT, using separation resolution provides a good initial metric of system performance.

A. Separation Resolution

In any imaging technology, resolution is an ambiguous concept. Classically, it refers to the ability of the imaging system to resolve two "point" targets that produce a scattered field of equal intensity. The resolution limit can be defined using Rayleigh's criterion [5], where two targets are considered resolved if the maximum value of the scattered spatial waveform pattern due to one target is at, or farther away than, the first minimum in the scattered waveform pattern of the other target [6]. Resolution beyond this limit is referred to as super-resolution [5], [7]. In inverse scattering problems, the Rayleigh (or base) resolution criterion may be generated via a linearization (*i.e.*, Born approximation) of the inverse scattering problem for idealized point targets. After the linearization of the inverse scattering problem, and using the Rayleigh criterion, the theoretically best possible

Manuscript received March 31, 2010; accepted April 22, 2010. Date of publication May 03, 2010; date of current version May 13, 2010. This work was supported by Western Economic Diversification Canada, the Natural Sciences and Engineering Research Council of Canada, CancerCare Manitoba, the University of Manitoba Graduate Fellowship, and Mathematics and Information Technology of Complex Systems Canada.

C. Gilmore is with Medical Physics, CancerCare Manitoba, Winnipeg, MB R3E 0V9, Canada (e-mail: colin.gilmore@cancercare.mb.ca).

P. Mojabi, A. Zakaria, and J. LoVetri are with the Department of Electrical and Computer Engineering, University of Manitoba, Winnipeg, MB R3T 5V6, Canada (e-mail: Joe_LoVetri@umanitoba.ca).

S. Pistorius is with Medical Physics, CancerCare Manitoba, Winnipeg, MB R3E 0V9, Canada, and also with the Department of Physics and Astronomy, University of Manitoba, Winnipeg, MB R3T 2N2, Canada.

Color versions of one or more of the figures in this letter are available online at <http://ieeexplore.ieee.org>.

Digital Object Identifier 10.1109/LAWP.2010.2049471

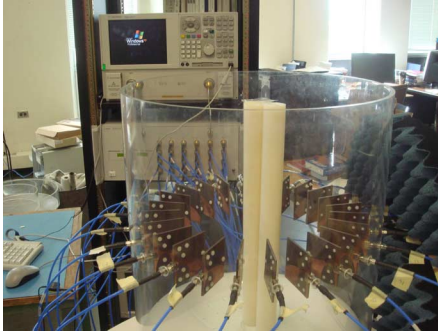


Fig. 1. The MWT system with two nylon cylinders.

resolution is $\lambda/2$ in the far field and $\lambda/4$ in the near field [1], where λ is the wavelength. In these linearization techniques, resolution beyond $\lambda/2$ is made possible by the collection and use of evanescent waves when the transmitters/receivers are located in the near field [1].

The use of nonlinear inverse scattering algorithms, which take into account multiple scattering events and penetration into a target, can improve resolution beyond these limits and can be even further improved through the placement of the transmit/receive elements in the near field. However, with a nonlinear inversion algorithm, a “point” target is no longer readily defined and imaged theoretically, thus some other target must be utilized. Some authors [7], [8] have resorted to the use of canonical circular targets, with maximum resolution defined as the minimum detectable separation between the two targets. We refer to this type of resolution with canonical targets as *separation resolution*. It is the nature of the nonlinear inverse scattering problem that no absolute (target-independent) resolution limit is definable; the resolution limit achieved is only applicable to those particular targets used. However, it does provide some indication of the resolving capabilities of the system, and provides a quantitative metric to measure system improvements or make comparisons between systems.

Under this definition, and using a ground-penetrating-radar-type data collection scheme, a resolution of $1/10$ of a wavelength with synthetic data [9] and a resolution of $\lambda/6$ with experimental data have been reported [7]. For biomedical applications, using a circular data collection configuration in a lossy background environment, a separation resolution of $\lambda/4$ has been reported [8]. Resolution well beyond this level is achievable, as we show herein.

II. METHODS

The details of our air-filled MWT imaging system have been previously reported in [4]. The system, pictured in Fig. 1, uses 24 Vivaldi antennas attached to network analyzer via a 24-port switch. Frequency-domain data is collected using a novel frequency selection process that minimizes the mutual coupling in the antenna array. Details of this process and the calibration procedure are described in [4]. As compared to what was reported in [4], the antennas have now been protected by a dielectric coating that is typically used for commercial circuit-board applications, and this has slightly changed the operating frequencies for the system. In this work, all imaging results are shown for data collected at a single frequency of 5 GHz, chosen using

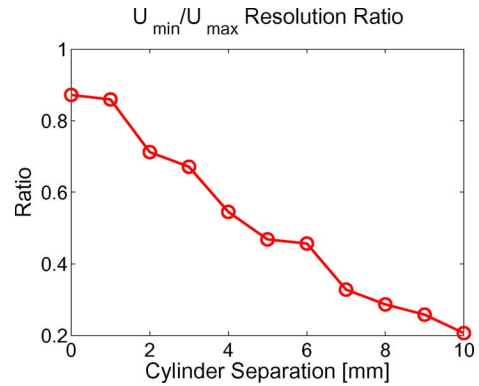


Fig. 2. Plot of the resolution ratio U_{\min}/U_{\max} for various separations of the two nylon cylinders.

the same process outlined in [4]. Similar to the work outlined in [7] and [8], we select two canonical targets each consisting of a nylon-66 cylinder 3.81 cm (1.5 inches) in diameter and 44 cm in height. At 5 GHz, the nylon has a complex relative permittivity of $\epsilon_r \approx 3.03 - j0.03$ (assuming a time dependency of $e^{j\omega t}$). Thus, the corresponding contrast is $\chi = (\epsilon - \epsilon_b)/\epsilon_b \approx 2.03 - j0.03$. Data were collected for 24 transmitters with 23 receivers operating for each transmitter (a total of 24×23 data points). The complete data-set was inverted using a multiplicatively regularized Gauss–Newton inversion technique described in [10], where the only prior information used was that of maintaining the reconstructed permittivity within physical bounds at each iteration (*i.e.*, $Re(\epsilon_r) \geq 1$ and $Im(\epsilon_r) \leq 0$).

The target, consisting of the two cylinders, was centered within the imaging system, and the separation of the two cylinders was varied from 0 (*i.e.*, touching) to 10 mm in 1-mm steps. To determine the separation resolution limit, a 1-D cross section of the real part of the reconstructed 2-D image is taken on a line running through the center of the two cylinders. Defining U_{\min} as the minimum pixel value on the 1-D cross-sectional image between the two targets, and U_{\max} as the first maximum closest to this minimum value, the ratio of the minimum pixel value to the maximum pixel value U_{\min}/U_{\max} is generated. Applying the Rayleigh criterion, if the ratio U_{\min}/U_{\max} is less than 0.81, then the cylinders are deemed to be resolved.

To emphasize that the obtained separation resolution limit has a high dependence on the target being imaged, the experiment was repeated with: 1) the same two nylon cylinders embedded in a polyvinyl chloride (PVC) cylinder; and 2) a significantly more complex phantom, the “e-phantom,” with multiple concave features. The e-phantom shape is shown in Fig. 5(a). For the first case, the two nylon cylinders (separated by 5 mm) were centered within a PVC cylinder with a wall thickness of ≈ 0.6 cm and an inside radius of ≈ 6.5 cm. Published values for the permittivity of PVC at 5 GHz are $\epsilon_r \approx 2.5 - j0.01$ [11]. The e-phantom is constructed of ultrahigh-molecular-weight (UHMW) polyethylene, and its dimensions are based on a similar phantom from [8]. The dielectric constant of UHMW polyethylene has been reported as $\epsilon_r = 2.3$, with negligible loss [12].

III. RESULTS

For the two nylon cylinders, the resolution ratio U_{\min}/U_{\max} is plotted in Fig. 2. Representative samples of the reconstructed

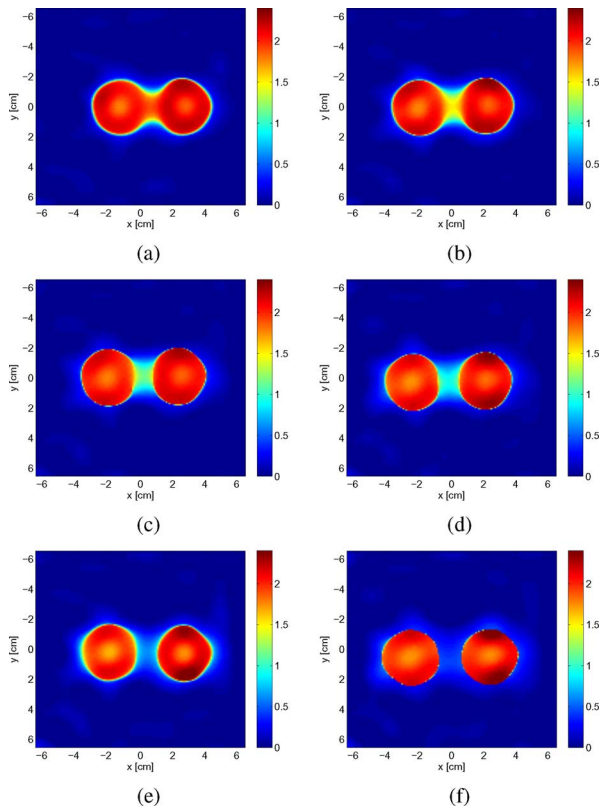


Fig. 3. Reconstruction of the two nylon-66 cylinders for separations of 0–10 mm in 2-mm steps. (a) 0 mm. (b) 2 mm. (c) 4 mm. (d) 6 mm. (e) 8 mm. (f) 10 mm.

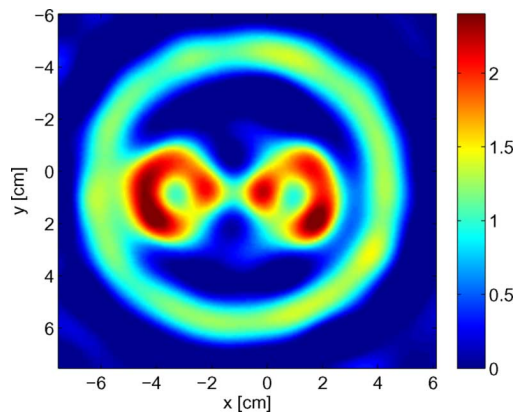


Fig. 4. Reconstruction of two nylon-66 cylinders embedded in a larger PVC cylinder. For this reconstruction, the two cylinders were separated by 5 mm.

images of the real part of the contrast for 0–10 mm in 2-mm steps are shown in Fig. 3. As the imaginary part of the contrast is very small in the cylinders, the reconstructions of the imaginary part of the contrast are not shown. By considering the directly collected data points, the two cylinders are resolved for all separations of 2 mm. We estimate a confidence interval of ± 0.4 mm due to errors in our positioning system.

The reconstruction of the contrast when the two cylinders are embedded in the PVC cylinder is shown in Fig. 4. In this case, the resolution ratio increases to 0.52 from a ratio of 0.47 when the cylinders were not embedded. Under the definition

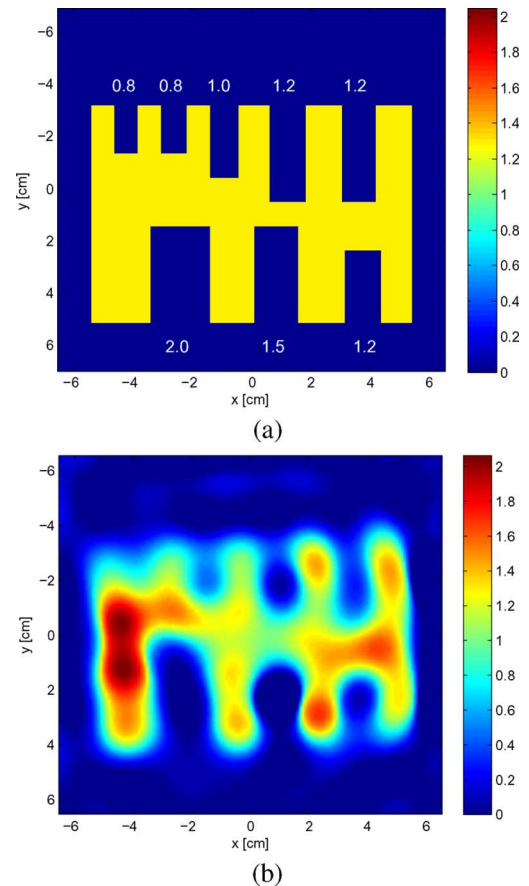


Fig. 5. Reconstruction of E-phantom. (a) The exact contrast of the phantom. The size of the gaps (in cm) is shown in white text above and below the gaps. (b) Reconstruction of the contrast.

of separation resolution limit used herein, the two cylinders are considered resolved; however, the inclusion of the PVC cylinder has clearly degraded the overall reconstruction of the nylon cylinders.

The reconstructed contrast for the e-phantom is shown in Fig. 5(b). Features with a minimum size of 1 cm and above are resolved, while the two concave features of 0.8 cm are not resolved.

IV. DISCUSSION

According to the results obtained with this experimental setup, a separation resolution of 2 mm has been achieved, which corresponds to a resolution of $\lambda/30$ at 5 GHz. This is a significant improvement over published experimental results using simple targets [7], [8] and highlights the potential for the technology. This high resolution is achieved through the collection and use of near-field data as well as the use of a nonlinear inversion algorithm that accounts for multiple scattering.

While we have resolved the targets at a separation of 2 mm, an inspection of Fig. 2 shows that the resolution limit should be at an even lower separation. A lower bound on the limiting separation resolution can be estimated to be 1.3 mm or $\approx \lambda/45$. This simple estimate assumes a linear variation in the resolution ratio between 1 and 2 mm and no errors in the positioning of the cylinders.

The use of the Rayleigh resolution criteria is qualitatively supported by observing the 0- and 2-mm separation reconstructions shown in Fig. 3. In the 0-mm reconstruction, the two cylinders are connected with a shaded region of a pixel value of ≈ 1.9 , while for the separated 2 mm reconstruction, the color switches to a lighter shade with a pixel value of ≈ 1.5 . We argue that, qualitatively, one would guess that the two cylinders are separated given the 2-mm reconstruction.

As expected, the resolution ratio shown in Fig. 2 reduces monotonically as the separation increases. However, it does not start from a value of 1.0 when the two cylinders are touching. This is due to variations in the reconstructed contrast throughout the cylinders, which raises the maximum pixel value in some regions within the cylinders (see, e.g., the slight rise in the right cylinder of the 0-mm reconstruction).

The reconstruction that includes the PVC cylinder (Fig. 4) shows one of the limitations in determining the separation resolution using the simplistic target environments considered herein. As expected when a PVC cylinder surrounds the target, the ratio of U_{\min}/U_{\max} increases, in this case by 11% from 0.47 to 0.52, which implies a reduction in separation resolution. The inclusion of the PVC cylinder also degrades the reconstruction of the nylon cylinders, to the point that they no longer appear as solid targets. The degradation is due to both: 1) a loss in the amount of useful energy interrogating the target (the PVC provides a significant barrier to the wave, which now must pass through the PVC wall twice before being detected by the antennas); and 2) an increase in the amount of multiple scattering present because of the presence of the surrounding cylinder.

The reconstruction of the e-phantom also shows the expected reduction in resolution abilities when imaging complicated targets. In this case, the concave features of the target create a particularly complex scattering environment, and the reduction of useful interrogating energy is not a factor. The two smallest features, of 0.8 cm ($\approx \lambda/8$) are not resolved. Features with a minimum width of 1.0 cm ($\approx \lambda/6$) and larger are resolved.

The use of a lossy matching fluid will also affect the achievable resolution because of the loss in the amount of interrogation energy available to the system. The use of a low-loss matching fluid will result in an increase in the multiple scattering produced at the boundaries of the MWT chamber. Thus, it is expected that the use of any matching fluid will deteriorate the achievable separation resolution.

While not the main focus of this letter, it is interesting to note that the diameters of the two cylinders are also reconstructed quite accurately (at least in the simple case with no PVC cylinder surrounding the target). For example, in the 10-mm separation reconstruction [Fig. 3(f)] the average reconstructed diameter of the nylon cylinders is 3.55 cm (calculated using the full-width at half-maximum criteria), an error of $\approx 7\%$, from the true diameter.

V. CONCLUSION

Using an air-filled, near-field experimental MWT system, combined with a multiplicative-regularized Gauss–Newton inversion algorithm, we have achieved a separation resolution of $\lambda/30$ for the case of two nylon cylinders imaged at 5 GHz. We have identified the drawbacks of using the separation resolution limit as an indicator of the expected resolution limit that might be achieved for biological targets and have exemplified two instances for which these drawbacks come into play. More complicated scatterers will no doubt reduce the achievable resolution, but we argue that the separation resolution is an effective means of quantitatively comparing various aspects of different MWT systems as well as quantifying improvements to any particular system.

ACKNOWLEDGMENT

The authors would like to acknowledge the support of M. Ostadrahimi with the antenna design of the system.

REFERENCES

- [1] T. J. Cui, W. C. Chew, X. X. Yin, and W. Hong, "Study of resolution and super resolution in electromagnetic imaging for half-space problems," *IEEE Trans. Antennas Propag.*, vol. 52, no. 6, pp. 1398–1411, Jun. 2004.
- [2] P. Meaney, K. Paulsen, A. Hartov, and R. Crane, "Microwave imaging for tissue assessment: Initial evaluation in multitarget tissue-equivalent phantoms," *IEEE Trans. Biomed. Eng.*, vol. 43, no. 9, pp. 878–890, Sep. 1996.
- [3] R. Halter, A. Hartov, and K. Paulsen, "A broadband high-frequency electrical impedance tomography system for breast imaging," *IEEE Trans. Biomed. Eng.*, vol. 55, no. 2, pp. 650–659, Feb. 2008.
- [4] C. Gilmore, P. Mojabi, A. Zakaria, M. Ostadrahimi, C. Kaye, S. Nogharian, L. Shafai, S. Pistorius, and J. LoVetri, "A wideband microwave tomography system with a novel frequency selection procedure," *IEEE Trans. Biomed. Eng.*, vol. 57, no. 4, pp. 894–904, Apr. 2010.
- [5] A. den Dekker and A. van den Bos, "Resolution: A survey," *J. Opt. Soc. Amer. A*, vol. 14, no. 3, pp. 547–557, 1997.
- [6] M. Born and E. Wolf, *Principles of Optics*, 7th ed. Cambridge, U.K.: Cambridge Univ. Press, 1999.
- [7] F. Chen and W. Chew, "Experimental verification of super resolution in nonlinear inverse scattering," *Appl. Phys. Lett.*, vol. 72, no. 23, pp. 3080–3082, 1998.
- [8] S. Semenov, R. Svenson, A. Bulyshev, A. Souvorov, A. Nazarov, Y. Sizov, V. Posukh, A. Pavlovsky, P. Repin, and G. Tatsis, "Spatial resolution of microwave tomography for detection of myocardial ischemia and infarction-experimental study on two-dimensional models," *IEEE Trans. Microw. Theory Tech.*, vol. 48, no. 4, pp. 538–544, Apr. 2000.
- [9] M. Moghaddam and W. Chew, "Nonlinear two-dimensional velocity profile inversion using time domain data," *IEEE Trans. Geosci. Remote Sens.*, vol. 30, no. 1, pp. 147–156, Jan. 1992.
- [10] P. Mojabi and J. LoVetri, "Microwave biomedical imaging using the multiplicative regularized gauss-newton inversion," *IEEE Antennas Wireless Propag. Lett.*, vol. 8, pp. 645–648, 2009.
- [11] K. Murata, A. Hanawa, and R. Nozaki, "Broadband complex permittivity measurement techniques of materials with thin configuration at microwave frequencies," *J. Appl. Phys.*, vol. 98, p. 084107, 2005.
- [12] W. S. Bigelow and E. G. Farr, "Impulse propagation measurements of the dielectric properties of several polymer resins," *Measurement Notes*, Note 55, pp. 1–52, 1999.